

# The weakened Weibel instability of collimated fast electron beam in nanotube array

L. LIAO,<sup>1</sup> R. ZHAO,<sup>1</sup> Y. BIE,<sup>2</sup> H. ZHANG,<sup>3</sup> AND C. HU<sup>1</sup>

<sup>1</sup>School of Materials Science and Engineering, Chongqing Jiaotong University, Chongqing 400074, People's Republic of China

<sup>2</sup>Nuclear and Radiation Safety Center, MEP, Beijing 100082, People's Republic of China

<sup>3</sup>College of Civil Engineering, Chongqing Jiaotong University, Chongqing 400074, People's Republic of China

(RECEIVED 11 October 2016; ACCEPTED 15 December 2016)

## Abstract

The Weibel instability of the collimated MeV fast electron beams in a nanotube array target is researched in this work. It is found that the filamentation of the fast electrons is significantly suppressed. When fast electrons propagate the nanotube array, a strong magnetic field is created near the surface of tubes to obstruct the transverse movement of the fast electrons and bend them into the inner vacuum spaces between the successive tubes. In consequence, the positive feedback loop between the magnetic field perturbation and the electrons density perturbation is broken and the Weibel instability is thus weakened. Furthermore, the calculated results by a hybrid particle-in-cell code have also proven this weakening effect on the Weibel instability. Because of the high-energy density delivered by the MeV electrons, these results indicate some significant applications in the high-energy physics, such as radiography, fast-electron beam focusing, and perhaps fast ignition.

**Keywords:** Fast electron beam; Nanotube array; Weibel instability

## 1. INTRODUCTION

When an intense laser pulse ( $>10^{18}$  W/cm<sup>2</sup>) irradiates a solid target, the light energy is deposited at the relativistic critical density, and then the relativistic electrons are produced (Perry & Mourou, 1994). These laser-driven fast electron beams constitute the mega-ampere currents and have been proposed that such a beam could be used in astrophysical plasmas (Gibbon, 2005), radiography (Park *et al.*, 2006), and fusion physics (Tabak *et al.*, 1994; Kodama *et al.*, 2001; Atzeni, 2003). When these relativistic electrons enter in a dense plasma, the return current is immediately generated in the background plasma for the demand of the charge neutrality. However, the return current is unstable for the Weibel instability, which will result in the filaments of the forward propagating fast electron beams and the fast growth of the magnetic field perturbation (Weibel, 1959; Sentoku *et al.*, 2000). These generated strong magnetic fields can significantly increase the divergence of the forward fast electrons. Lots of experimental and simulation works have shown that the fast electron beams from laser–matter interaction are generally of large divergence (40°–50°) (Sentoku *et al.*,

2000; Santos *et al.*, 2002; Kodama *et al.*, 2004a; Stephens *et al.*, 2004; Lancaster *et al.*, 2007; Green *et al.*, 2008). To lower the fast electron divergence, the control of the relativistic fast electrons has been studied extensively (Borghesi *et al.*, 1999; Campbell *et al.*, 2003; Danson *et al.*, 2004; Nakamura *et al.*, 2007; Robinson & Sherlock, 2007; Robinson *et al.*, 2008a, b; Kar *et al.*, 2009).

Recently, the experimental works performed on the carbon nanotube (CNT) array have shown the novel transportation of the fast electrons in CNT. The collimated fast electron transportation over a macroscopic (millimeter) distance (about 100 times longer than the typical filamentation length) has been observed in the CNT array (Ji *et al.*, 2010; Chatterjee *et al.*, 2012; Liao *et al.*, 2013; Liao *et al.*, 2014). These experimental results indicate that the CNT array can effectively suppress the Weibel instability of the fast electron beams. Otherwise, the mega-ampere intensity cannot sustain as long as a millimeter.

Recently, Mishra *et al.* (2014) present an approach to achieve the suppression of the Weibel instability by periodically modifying the electron density of the background with the equilibrium density ripples shorter than the skin depth. It is pointed out that the CNT target is exactly the periodic structure with the density ripples and the observed collimated fast electron transportations are the direct consequence of the

Address correspondence and reprint requests to: R. Zhao, School of Materials Science and Engineering, Chongqing Jiaotong University, Chongqing 400074, People's Republic of China. E-mail: [rqzhao@cqjtu.edu.cn](mailto:rqzhao@cqjtu.edu.cn)

weakened Weibel instability by the periodic density ripples of the CNT array. However, they give these results by a linearized two stream fluid model. For the electrons in the CNT array structure, the density variation is not a weak ripple but a huge density variation (from zero density of the vacuum to the electron density of the CNT in a period). It is not appropriate to apply the linearized perturbation model on the CNT array.

In the present work, we research the filamentation of the fast electron beams in a nanotube array and the growth of the magnetic field by a hybrid-particle-in-cell simulation. It is found that the CNT array can effectively weaken the Weibel instability and the explanation of the over millimeter distance of the fast electrons transportation recently found in CNT array has been given (Ji *et al.*, 2010; Chatterjee *et al.*, 2012; Liao *et al.*, 2013, 2014). The self-generated magnetic field and electric field near the surface of the tubes play the essential role. The electric field draws the fast electrons into the tube, but the magnetic field pulls them out, and these two forces will reach equilibrium near the tube surface (Kodama *et al.*, 2004b). It makes most of the fast electrons propagate near the tube surfaces, and they could hardly move across the tubes. As the inner spaces between the successive tubes are very short, this effect makes the spaces play as “traps”. The fast electrons are confined into these inner spaces, and their transverse dispersion is impeded. In the absence of the transverse movement of the fast electrons, the filamentation loses the supplies of the fast electrons and cannot develop forward. As a result, the Weibel instability is stabilized.

## 2. THEORY AND DISCUSSION

The generation of the magnetic field during the propagation of the fast electrons through a solid target can be described by combining a simple Ohm’s law  $\vec{E} = -\eta\vec{j}_f$ , with Faraday’s law to yield

$$\frac{\partial \vec{B}}{\partial t} = \eta \nabla \times \vec{j}_f + (\nabla \eta) \times \vec{j}_f, \quad (1)$$

where  $\eta$  is the resistivity, and  $\vec{j}_f$  is the fast-electron current density. The first term on the right-hand side generates a magnetic field that pushes the fast electrons toward to the region where possesses a higher fast-electron current density, while the second term pushes the fast electrons toward to the region where possesses the higher resistivity. Moreover, the first term is the origin of the magnetic instability. Giving a ripple of the fast-electron current density, normal to the streaming direction, the generated field by the first term would enhance the current density ripples. The fast electrons are pushed into the high-density region by the magnetic field, and the generated field gets further stronger. As a result, the significant filamentation of the fast electrons is formed.

For the tube array, the inner spaces between tubes are vacuum, whose  $\eta$  is infinitely large, but the  $\eta$  of plasma in

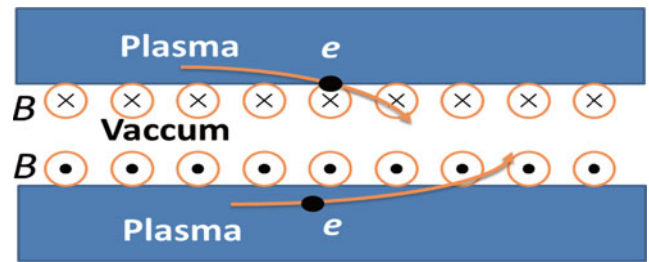


Fig. 1. The plot of the magnetic field at the CNT surfaces.

tubes is finite. Therefore, at the surface of the tubes, that is, the interface between the vacuum and the plasma, the gradient of the resistivity is very large and the generated field by the second terms of Eq. (1) is dominated. During the propagation of intense fast electron flux along the tubes, the fast electron beams are bent into the vacuum region by the magnetic field as depicted in Figure 1. In the transverse direction (normal to the tubes), these inner spaces act as the magnetic traps and the fast electrons are confined in these regions to propagate forward. Without enough transverse kinetic energy or force on the fast electrons, these electrons cannot escape from the magnetic traps.

Considering there existing a magnetic perturbation in the transverse direction. Because of the second term of Eq. (1), the transverse movement of these fast electrons is impeded by the magnetic field near the surfaces and the fast electrons are difficult to move across one tube to another. If the perturbation is larger than the aligning period of the tubes, the growing rate of the perturbation would be suppressed. For the perturbations smaller than the tube width, it is a well-known fact that the transverse electromagnetic perturbations are also weakened if the perturbations are shorter than the skin depth (Mishra *et al.*, 2014) (i.e.,  $ck/\omega_{pe} > 1$ ). Therefore, if the tube width is not larger than the skin depth, the magnetic instability is also suppressed. For a tube array, the inner magnetic instability (with large  $k$  and small size) can be suppressed by decreasing the tube width, while the magnetic instability across the tubes (with small  $k$  and large size) can be suppressed by increasing the resistive magnetic field at the tube surface.

## 3. NUMERICAL RESULTS AND DISCUSSION

For a further quantitative investigation, the numerical calculation is required. For a comparison’s purpose, the growth of the instability in a bulk carbon target and the CNT array structure are both numerically modeled by a hybrid algorithm that means a code using a particle-in-cell algorithm to describe the kinetic fast electrons, where the background electrons are treated as a Spitzer resistive conductor (Spitzer & Harm, 1953; Robinson & Sherlock, 2007; Robinson *et al.*, 2008a, b). Because of the intense background return current induced by the fast electrons, the backgrounds are ionized into plasma by the Ohm heating in a short time. The

ionization process is thus not taken into consideration and we assume that the background is instantaneously ionized and heated to 100 eV on the fast electrons arriving. Hence, we use the Spitzer resistivity model of the hot plasma for the background (Spitzer & Harm, 1953):

$$\eta = 10^{-4} Z \ln \Lambda / T_c^{1.5}, \tag{2}$$

where  $T_c$  is the temperature of the cold electrons (in eV). The Ohm heating of the background plasma gives:

$$\frac{\partial T_c}{\partial t} = \frac{\eta j_c^2}{C}, \tag{3}$$

where  $C$  is the heat capacity of the cold electron specified by the ideal gas heat capacity:  $C = 1.5 n_c$  where  $n_c$  and  $j_c$  is the density and the current of the cold electron. Here,  $j_c$  gives by generalized the Ohm law ignoring the heat pressure and the inertia term:

$$\vec{j}_c = (\vec{E} - \frac{\vec{j}_c \times \vec{B}}{en}) / \eta. \tag{4}$$

The simulations are carried out in a domain of  $6.0 \mu\text{m} \times 6.0 \mu\text{m}$  ( $x \times y$ ), represented by a  $4096 \times 4096$  grids. The CNT target is modeled by a group of tubes periodically aligning in the  $y$ -direction (the tube width is 50 nm and the space

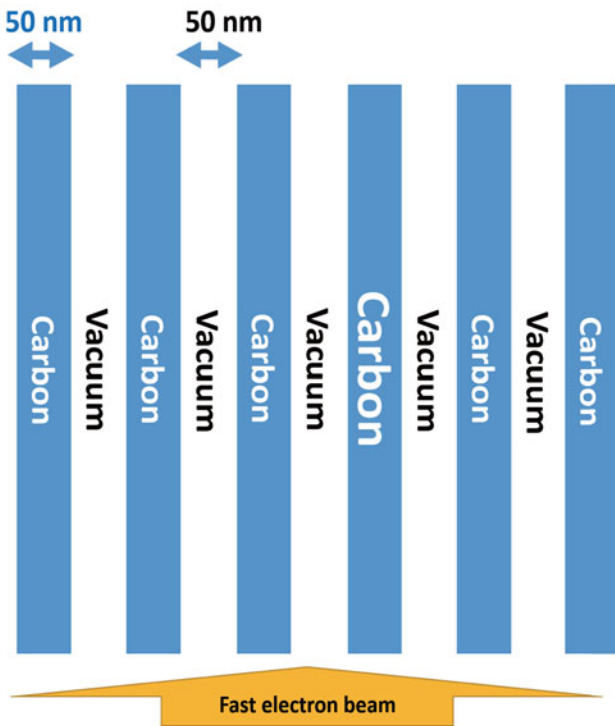


**Fig. 2.** The plot of the CNT array structure. The blue color presents carbon regions and the white color present the vacuum regions. The tube width is 50 nm and the space between the successive tubes is also 50 nm. The fast electrons are uniformly injected from the bottom of the box with an average energy of 2.0 MeV.

between the successive tubes is also 50 nm,  $ck/\omega_{pc} \approx 5$  for one single tube) as shown in Figure 2. The fast electron density in the tubes is set to  $1.0 \times 10^{22} \text{ cm}^{-3}$  but zero for the inner spaces. These fast electrons are uniformly injected from the bottom of the box. The initial fast-electron energetic distribution is set as the Maxwellian of temperature:  $kT = 2.0 \text{ MeV}$  and the initial velocity is along the  $y$ -axis. The electron density inside the tubes is chosen to be  $6.0 \times 10^{23} \text{ cm}^{-3}$ . The cold electrons in the background are assumed to be pre-heated to 100 eV.

By this model, we first simulate the evolution of the fast electrons in a bulk carbon plasma. The evolution of the fast electron distribution is contained in Figure 3, which illustrates a significant filamentation of the fast electrons. Figure 4 shows the evolution of the self-generated magnetic field. The mechanism of the Weibel instability is well known. While the fast electrons propagate in the uniform plasma, a return cold electron beam with an equal current is created and the equilibrium with two counter beams is formed. Giving a density ripple in the fast electron beam, normal to the streaming

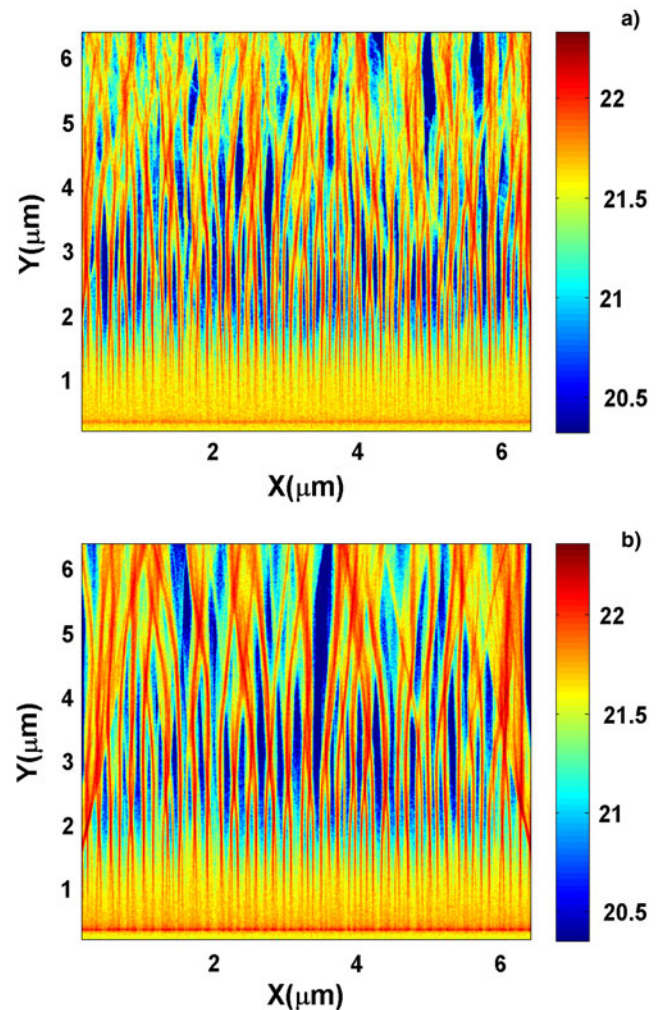


**Fig. 3.** The log10 plot of the fast electron density in a bulk carbon target in: (a) at 25 fs and (b) at 100 fs.

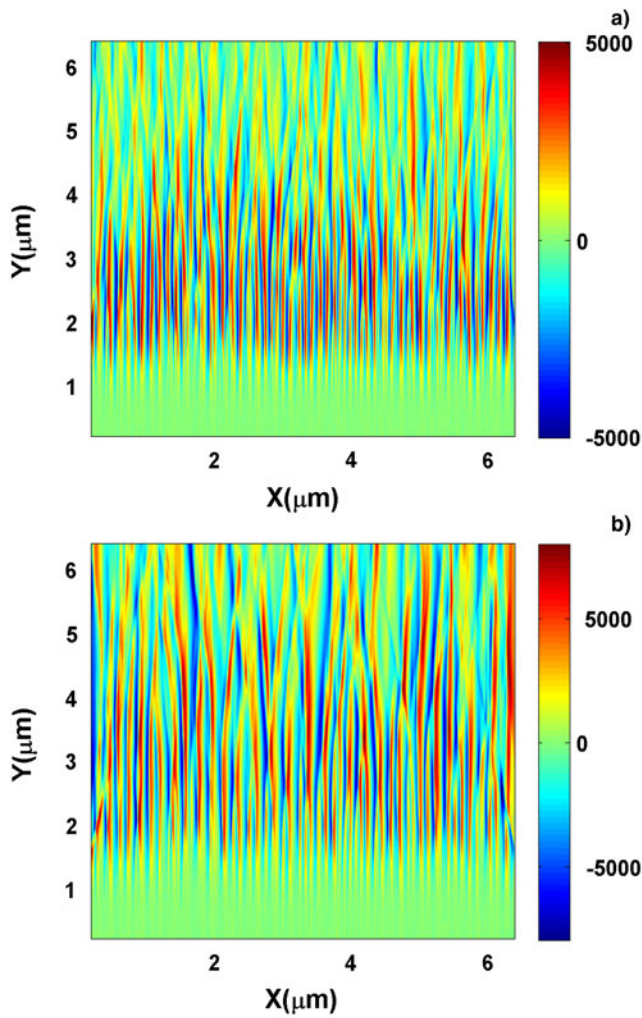


Fig. 4. The plots of the self-generated magnetic field in the bulk carbon target in: (a) at 25 fs and (b) at 100 fs.

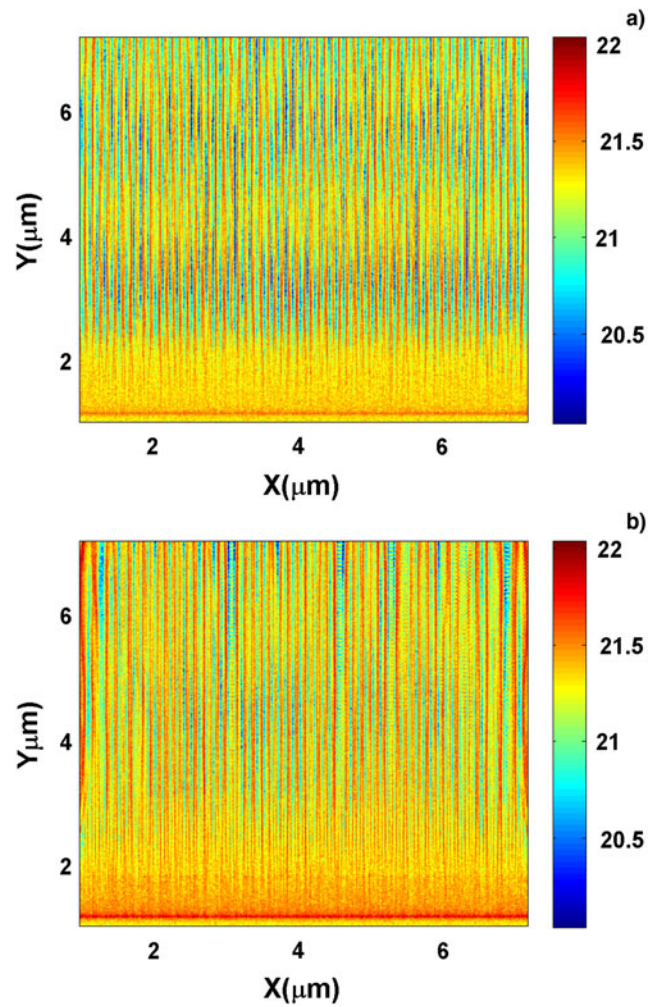


Fig. 5. The log10 plot of fast electron density in the CNT array in: (a) at 25 fs and (b) at 100 fs.

direction, it leads to a magnetic field, which repulses the return current out of the high-density region and reinforces the magnetic field again, by which, more and more fast electrons are gathered in the high-density region, thus providing a positive feedback responsible for the current sheet separation as depicted in Figure 3 and a very strong self-generated magnetic field as shown in Figure 4. It is clear that the transverse movement of the electrons driven by the magnetic field plays an essential role. If the transverse movement of the electrons is stopped, the Weibel instability will be weakened.

The self-generated field in the CNT array can effectively stop the transverse movement of the fast electrons. Thus, the stabilization of the Weibel instability in this structure can be expected. Figure 5 gives the calculated fast electron distribution in the CNT array and Figure 6 shows the generated magnetic field. As these fast electrons enter the CNT array, a pair of the self-generated magnetic fields will create in the inner spaces between the successive tubes because of the strong mismatch of matter-vacuum at tube surface. Both these magnetic fields act to push the fast

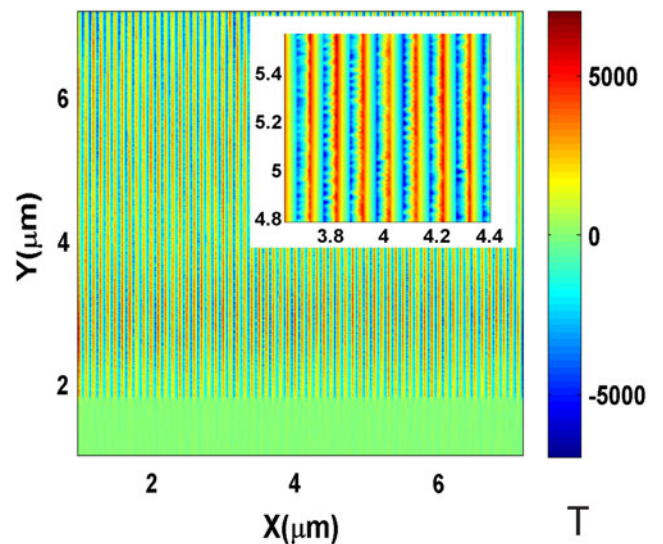


Fig. 6. The plot of the magnetic field in the CNT array at 25 fs. The inserted figure shows the details of the magnetic field in the tubes and the inner spaces.

electrons into the inner spaces between the successive tubes. As a result, the fast electrons mainly propagate in the inner spaces. These magnetic fields act as a magnetic “trap” to trap the fast electrons in the inner spaces, by which, the transverse movement of the fast electrons is significantly suppressed. If there the fast-electron density ripples exist, the induced magnetic field cannot conquer the magnetic “trap” to push more fast electrons into the high-density region. It weakens the positive feedback between the magnetic field perturbation and the electrons density perturbation. Consequently, the magnetic field cannot grow strong enough to separate the current sheet as in bulk carbon background. Moreover, because of the tube diameter shorter than the skin depth, the transverse electromagnetic perturbation is also weakened and there is no current sheet separation happens in the tubes. Consequently, either for the whole tube array or a single tube, the growth of the Weibel instability in the CNT is significantly weakened.

#### 4. CONCLUSION

In summary, we have researched the evolution of the fast electrons’ filamentation in the CNT array by a hybrid particle-in-cell simulation and found that the self-generated magnetic field act to trap the fast electrons in the inner spaces between the successive tubes. It prevents the fast electrons move from one tube to others in the transverse direction, and thus breaks the positive feedback loop between the magnetic field perturbation and the electrons density perturbation. As a result, the fast electron filamentation and the Weibel instability are weakened. We believe that other similar nanotube array structures such as ZnO, Cu, and Au nanorod arrays can also weaken the Weibel instability as well as the CNT array. Because of the high-energy density delivered by the MeV electrons, these results indicate some specific applications in the high-energy physics, such as radiography, fast-electron beam focusing, and perhaps fast ignition.

#### ACKNOWLEDGEMENTS

This work was supported by the National Natural Science Foundation of China (Grant Nos 11404045 and 11304407).

#### REFERENCES

- ATZENI, S., M.-T.-V.J. (2003). *Inertial Fusion-Beam Plasma Interaction, Hydrodynamic, Dense Plasma Physics*. Oxford: Clarendon.
- BORGHESI, M., MACKINNON, A.J., BELL, A.R., MALKA, G., VICKERS, C., WILLI, O., DAVIES, J.R., PUKHOV, A. & MEYER-TER-VEHN, J. (1999). Observations of collimated ionization channels in aluminum-coated glass targets irradiated by ultraintense laser pulses. *Phys. Rev. Lett.* **83**, 4309–4312.
- CAMPBELL, R.B., DEGROOT, J.S., MEHLHORN, T.A., WELCH, D.R. & OLIVER, B.V. (2003). Collimation of PetaWatt laser-generated relativistic electron beams propagating through solid matter. *Phys. Plasmas* **10**, 4169–4172.
- CHATTERJEE, G., SINGH, P.K., AHMED, S., ROBINSON, A.P.L., LAD, A.D., MONDAL, S., NARAYANAN, V., SRIVASTAVA, I., KORATKAR, N., PASLEY, J., SOOD, A.K. & KUMAR, G.R. (2012). Macroscopic transport of mega-ampere electron currents in aligned carbon-nanotube arrays. *Phys. Rev. Lett.* **108**, 235005.
- DANSON, C.N., BRUMMITT, P.A., CLARKE, R.J., COLLIER, J.L., FELL, B., FRACKIEWICZ, A., HANCOCK, S., HAWKES, S., HERNANDEZ-GOMEZ, C., HOLLIGAN, P., HUTCHINSON, M.H.R., KIDD, A., LESTER, W.J., MUSGRAVE, I.O., NEELY, D., NEVILLE, D.R., NORREYS, P.A., PEPLER, D.A., REASON, C.J., SHAIKH, W., WINSTONE, T.B., WYATT, R.W.W. & WYBORN, B.E. (2004). Vulcan Petawatt – an ultra-high-intensity interaction facility. *Nucl. Fusion* **44**, S239–S246.
- GIBBON, P. (2005). *Short Pulse Laser Interactions with Matter: an Introduction*. London: College Press.
- GREEN, J.S., OVCHINNIKOV, V.M., EVANS, R.G., AKLI, K.U., AZECHI, H., BEG, F.N., BELLEI, C., FREEMAN, R.R., HABARA, H., HEATHCOTE, R., KEY, M.H., KING, J.A., LANCASTER, K.L., LOPES, N.C., MA, T., MACKINNON, A.J., MARKEY, K., MCPHEE, A., NAJMUDIN, Z., NILSON, P., ONOFREI, R., STEPHENS, R., TAKEDA, K., TANAKA, K.A., THEOBALD, W., TANIMOTO, T., WAUGH, J., VAN WOERKOM, L., WOOLSEY, N.C., ZEPF, M., DAVIES, J.R. & NORREYS, P.A. (2008). Effect of laser intensity on fast-electron-beam divergence in solid-density plasmas. *Phys. Rev. Lett.* **100**, 015003.
- Ji, Y.L., JIANG, G., WU, W.D., WANG, C.Y., GU, Y.Q. & TANG, Y.J. (2010). Efficient generation and transportation of energetic electrons in a carbon nanotube array target. *Appl. Phys. Lett.* **96**, 041504.
- KAR, S., ROBINSON, A.P.L., CARROLL, D.C., LUNDH, O., MARKEY, K., MCKENNA, P., NORREYS, P. & ZEPF, M. (2009). Guiding of relativistic electron beams in solid targets by resistively controlled magnetic fields. *Phys. Rev. Lett.* **102**, 055001.
- KODAMA, R., AZECHI, H., FUJITA, H., HABARA, H., IZAWA, Y., JITSUNO, T., JOZAKI, T., KITAGAWA, Y., KRUSHELNICK, K., MATSUOKA, T., MIMA, K., MIYANAGA, N., NAGAI, K., NAGATOMO, H., NAKAI, M., NISHIMURA, H., NORIMATSU, T., NORREYS, P., SHIGEMORI, K., SHIRAGA, H., SUNAHARA, A., TANAKA, K.A., TANPO, M., TOYAMA, Y., TSUBAKIMOTO, K., YAMANAKA, T. & ZEPF, M. (2004a). Fast plasma heating in a cone-attached geometry – towards fusion ignition. *Nucl. Fusion* **44**, S276–S283.
- KODAMA, R., NORREYS, P.A., MIMA, K., DANGOR, A.E., EVANS, R.G., FUJITA, H., KITAGAWA, Y., KRUSHELNICK, K., MIYAKOSHI, T., MIYANAGA, N., NORIMATSU, T., ROSE, S.J., SHOZAKI, T., SHIGEMORI, K., SUNAHARA, A., TAMPO, M., TANAKA, K.A., TOYAMA, Y., YAMANAKA, Y. & ZEPF, M. (2001). Fast heating of ultrahigh-density plasma as a step towards laser fusion ignition. *Nature* **412**, 798–802.
- KODAMA, R., SENTOKU, Y., CHEN, Z.L., KUMAR, G.R., HATCHETT, S.P., TOYAMA, Y., COWAN, T.E., FREEMAN, R.R., FUCHS, J., IZAWA, Y., KEY, M.H., KITAGAWA, Y., KONDO, K., MATSUOKA, T., NAKAMURA, H., NAKATSUTSUMI, M., NORREYS, P.A., NORIMATSU, T., SNAVELY, R.A., STEPHENS, R.B., TAMPO, M., TANAKA, K.A. & YABUCHI, T. (2004b). Plasma devices to guide and collimate a high density of MeV electrons. *Nature* **432**, 1005–1008.
- LANCASTER, K.L., GREEN, J.S., HEY, D.S., AKLI, K.U., DAVIES, J.R., CLARKE, R.J., FREEMAN, R.R., HABARA, H., KEY, M.H., KODAMA, R., KRUSHELNICK, K., MURPHY, C.D., NAKATSUTSUMI, M., SIMPSON, P., STEPHENS, R., STOECKL, C., YABUCHI, T., ZEPF, M. & NORREYS, P.A. (2007). Measurements of energy transport

- patterns in solid density laser plasma interactions at intensities of  $5 \times 10^{20} \text{ W cm}^{-2}$ . *Phys. Rev. Lett.* **98**, 125002.
- LIAO, L., WU, W.D., GU, Y.Q., ZHOU, W.M., WANG, C.Y., FU, Z.B., YANG, X. & TANG, Y.J. (2013). Production of collimated MeV electron beam in carbon nanotube array irradiated by super-intense femtosecond laser. *Carbon* **65**, 28–34.
- LIAO, L., WU, W.D., WANG, C.Y., ZHOU, M.J., FU, Z.B. & TANG, Y.J. (2014). The collimation of intense relativistic electron beams generated by ultra-intense femtosecond laser in nanometer-scale solid fiber array. *Appl. Phys. Lett.* **104**, 083520.
- MISHRA, S.K., KAW, P., DAS, A., SENGUPTA, S. & KUMAR, G.R. (2014). Stabilization of beam-Weibel instability by equilibrium density ripples. *Phys. Plasmas* **21**, 012108.
- NAKAMURA, T., SAKAGAMI, H., JOHZAKI, T., NAGATOMO, H., MIMA, K. & KOGA, J. (2007). Optimization of cone target geometry for fast ignition. *Phys. Plasmas* **14**, 103105.
- PARK, H.S., CHAMBERS, D.M., CHUNG, H.K., CLARKE, R.J., EAGLETON, R., GIRALDEZ, E., GOLDSACK, T., HEATHCOTE, R., IZUMI, N., KEY, M.H., KING, J.A., KOCH, J.A., LANDEN, O.L., NIKROO, A., PATEL, P.K., PRICE, D.F., REMINGTON, B.A., ROBNEY, H.F., SNAVELY, R.A., STEINMAN, D.A., STEPHENS, R.B., STOECKL, C., STORM, M., TABAK, M., THEOBALD, W., TOWN, R.P.J., WICKERSHAM, J.E. & ZHANG, B.B. (2006). High-energy K alpha radiography using high-intensity, short-pulse lasers. *Phys. Plasmas* **13**, 056309.
- PERRY, M.D. & MOUROU, G. (1994). Terawatt to petawatt subpicosecond lasers. *Science* **264**, 917–924.
- ROBINSON, A.P.L., KINGHAM, R.J., RIDGERS, C.P. & SHERLOCK, M. (2008a). Effect of transverse density modulations on fast electron transport in dense plasmas. *Plasma Phys. Control. Fusion* **50**, 065019.
- ROBINSON, A.P.L. & SHERLOCK, M. (2007). Magnetic collimation of fast electrons produced by ultraintense laser irradiation by structuring the target composition. *Phys. Plasmas* **14**, 083105.
- ROBINSON, A.P.L., SHERLOCK, M. & NORREYS, P.A. (2008b). Artificial collimation of fast-electron beams with two laser pulses. *Phys. Rev. Lett.* **100**, 025002.
- SANTOS, J.J., AMIRANOFF, F., BATON, S.D., GREMILLET, L., KOENIG, M., MARTINOLLI, E., LE GLOAHEC, M.R., ROUSSEAU, C., BATANI, D., BERNARDINELLO, A., GREISON, G. & HALL, T. (2002). Fast electron transport in ultraintense laser pulse interaction with solid targets by rear-side self-radiation diagnostics. *Phys. Rev. Lett.* **89**, 207–213.
- SENTOKU, Y., MIMA, K., KOJIMA, S. & RUHL, H. (2000). Magnetic instability by the relativistic laser pulses in overdense plasmas. *Phys. Plasmas* **7**, 689–695.
- SPITZER, L. & HARM, R. (1953). Transport phenomena in a completely ionized gas. *Phys. Rev.* **89**, 977–981.
- STEPHENS, R.B., SNAVELY, R.A., AGLITSKIY, Y., AMIRANOFF, F., ANDERSEN, C., BATANI, D., BATON, S.D., COWAN, T., FREEMAN, R.R., HALL, T., HATCHETT, S.P., HILL, J.M., KEY, M.H., KING, J.A., KOCH, J.A., KOENIG, M., MACKINNON, A.J., LANCASTER, K.L., MARTINOLLI, E., NORREYS, P., PERELLI-CIPPO, E., LE GLOAHEC, M.R., ROUSSEAU, C., SANTOS, J.J. & SCIANITTI, F. (2004). K-alpha fluorescence measurement of relativistic electron transport in the context of fast ignition. *Phys. Rev. E* **69**, 039901.
- TABAK, M., HAMMER, J., GLINSKY, M.E., KRUEER, W.L., WILKS, S.C., WOODWORTH, J., CAMPBELL, E.M., PERRY, M.D. & MASON, R.J. (1994). Ignition and high-gain with ultrapowerful lasers. *Phys. Plasmas* **1**, 1626–1634.
- WEIBEL, E.S. (1959). Spontaneously growing transverse waves in a plasma due to an anisotropic velocity distribution. *Phys. Rev. Lett.* **2**, 83–84.